

July 13, 2023

QCD effective charges from low-energy neutrino structure functions

TANJONA R. RABEMANANJARA

*Department of Physics and Astronomy, Vrije Universiteit, NL-1081 HV Amsterdam
Nikhef Theory Group, Science Park 105, 1098 XG Amsterdam, The Netherlands*

We present a new perspective on the study of the behavior of the strong coupling $\alpha_s(Q^2)$ – the fundamental coupling underlying the interactions between quarks and gluons as described by the Quantum Chromodynamics (QCD) – in the low-energy infrared (IR) regime. We rely on the NNSF ν determination of neutrino-nucleus structure functions valid for all values of Q^2 from the photoproduction to the high-energy region to define an effective charge following the the Gross-Llewellyn Smith (GLS) sum rule. As a validation, our predictions for the low-energy QCD effective charge are compared to experimental measurements provided by JLab.

PRESENTED AT

DIS2023: XXX International Workshop on Deep-Inelastic
Scattering and Related Subjects,
Michigan State University, USA, 27-31 March 2023



Introduction. The study of (anti-)neutrino-nucleus interactions plays a crucial role in the interpretation of ongoing and future neutrino experiments which ultimately will also help improve our general understanding of the strong interactions as described by Quantum Chromodynamics (or QCD in short). Different types of interactions occur depending on the neutrino energies E_ν probed. The one of particular relevance to QCD is inelastic neutrino scattering, which occurs at energies above the resonance region, for $E_\nu \gtrsim \mathcal{O}(10)$ GeV and when the invariant mass of the final states satisfies $W \gtrsim 2$ GeV. In such a regime, the inelastic neutrino scattering is composed of nonperturbative and perturbative regimes referred to as shallow-inelastic scattering (SIS) and deep-inelastic scattering (DIS), respectively.

The main observables of interest in neutrino inelastic scattering are the differential cross-sections which are expressed directly as linear combinations of structure functions $F_{i,A}^{\nu/\bar{\nu}}(x, Q^2)$ with x the Bjorken variable, Q^2 the momentum transfer, and A the atomic mass number of the proton/nuclear target. In the DIS regime, the neutrino structure functions are factorized as a convolution between the parton distribution functions (PDFs) and hard-partonic cross-sections. The latter are calculable to high order in perturbation theory while the former have to be extracted from experimental data. On the other hand, in the SIS regime in which nonperturbative effects dominate, theoretical predictions of neutrino structure functions do not admit a factorised expressions in terms of PDFs. Various theoretical frameworks have been developed to model these low- Q^2 neutrino structure functions, e.g. [1], but all of them present limitations.

In [2] we presented the first determination of neutrino-nucleus structure functions and their associated uncertainties that is valid across the entire range of Q^2 relevant for neutrino phenomenology, dubbed NNSF ν . The general strategy comes down to dividing the Q^2 range into three distinct but interconnected regions. These regions refer respectively to the low-, intermediate-, and large-momentum transfers. At low momentum transfers $Q^2 \lesssim Q_{\text{dat}}^2$ in which nonperturbative effects occur, we parametrize the structure functions in terms of neural networks (NN) based on the information provided by experimental measurements following the NNPDF approach [3]. In the intermediate momentum transfer regions, $Q_{\text{dat}}^2 \lesssim Q \lesssim Q_{\text{thr}}^2$, the NN is fitted to the DIS predictions for convergence. And finally at large momentum transfers, $Q \gtrsim Q_{\text{dat}}^2$, the NN predictions are replaced by the pure DIS perturbative computations.

Such a framework allows us to provide more reliable predictions of the low-energy neutrino structure functions – we refer the reader to [2] for more details. The NNSF ν enables the robust, model-independent evaluation of inclusive inelastic neutrino cross-sections for energies from a few tens of GeV up to the several EeV relevant for astroparticle physics [4], and in particular fully covers the kinematics of present [5, 6] and future [7, 8] LHC neutrino experiments.

Aside from its relevance in studying neutrino physics, the NNSF ν framework may also potentially be used as a tool to strengthen our understanding of the nonperturbative regions of QCD owing to its predictions in the low-energy regime. It is commonly understood that studying the theory of the strong interactions in the Infrared (IR) regime is necessary to understand both high-energy and hadronic phenomena therefore providing sensitivity to a variety of Beyond the Standard Model (BSM) scenarios. One aspect that deserves a closer look in studying long-range QCD dynamics is the behavior of the strong coupling α_s due to its special property as an expansion parameter for first-principle calculations. In the perturbative regime, the uncertainties in the value of α_s is known to the sub-percent level ($\Delta\alpha_s/\alpha_s = 0.85\%$, [9, 10]). At low- Q^2 , however, its determination is subject to large uncertainties mainly due to the lack of theoretical frameworks that can correctly accommodate for the nonperturbative effects.

A number of approaches have been explored in the literature to study the coupling in

the nonperturbative regime including lattice QCD or the Anti-de-Sitter/Conformal Field Theory (AdS/CFT) duality implemented using QCD's light-front quantization. In the following, we use the Grunberg's effective charge approach defined from the Gross-Llewellyn Smith sum rule. From perturbative QCD, the effective coupling charge can be calculated from the perturbative series of an observable – usually defined in terms of the sum rules – truncated to its first order in α_s . The reason for such a truncation is related to the scheme as at leading order the observable is independent of the renormalization scheme (RS). One of the main advantages of the effective charge w.r.t. different approaches is that there are several experiments that measure the effective coupling $\alpha_s^{\text{eff}}(Q^2)$ to compare the theoretical computations to.

Here first we briefly review the Gross-Llewellyn Smith sum rule and verify that it is satisfied using the neutrino structure function predictions from the NNSF ν determination. We then use the NNSF ν framework to compute the effective charge defined from the sum rule and compare the results to experimental measurements extracted at JLab [11–14].

The Gross-Llewellyn Smith sum rule. The neutrino structure function $x F_3^{\nu N}$ must satisfy the Gross-Llewellyn Smith (GLS) sum rule [15] in which its unsubtracted dispersion relation has to be equal to the number of valence quarks inside the nucleon N . Such a dispersion relation could also be extended to the neutrino-nucleus interactions in which the GLS sum rule writes as follows:

$$\text{GLS}(Q^2, A) \equiv \frac{1}{2} \int_0^1 dx (F_3^{\nu A} + F_3^{\bar{\nu} A}) (x, Q^2) = 3 \left(1 + \sum_{k=1}^3 \left(\frac{\alpha_s(Q^2)}{\pi} \right)^k c_k(n_f) \right) + \frac{\Delta^{\text{HT}}}{Q^2}, \quad (1)$$

where n_f is the number of active flavors at the scale Q^2 . The terms inside the parentheses on the right-hand side represent the perturbative contribution to the leading-twist part whose coefficients c_k have been computed up to $\mathcal{O}(\alpha_s^4)$. The Δ^{HT} -term instead represents the power suppressed non-perturbative corrections, see [16] for a recent review. Notice that the form of the perturbative part in Eq. (1) is convenient because, as opposed to many observables in pQCD, it does not depend both on x and on the mass number A .

The low-energy experimental data from which the NNSF ν neutrino structure functions were determined do not provide measurements in the low- x region, and therefore the evaluation of Eq. (1) largely depends on the modeling of the small- x extrapolation region. In our predictions, the behavior at small- x is inferred from the medium- large- x regions via the preprocessing factor $x^{1-\alpha_i}$ whose exponents are fitted to the data. In addition, due to the large uncertainties governing the small- x region, we have to truncate the integration at some x_{min} value. The truncated sum rule should however converge to the pQCD predictions in the limit $x \rightarrow 0$. The truncated sum rule writes as

$$\text{GLS}(Q^2, A, x_{\text{min}}) \equiv \frac{1}{2} \int_{x_{\text{min}}}^1 dx (F_3^{\nu A} + F_3^{\bar{\nu} A}) (x, Q^2), \quad (2)$$

for different values of the lower integration limit x_{min} and different nucleon/nuclear targets.

In Fig. 1 we display the results of computing the truncated GLS sum rule in Eq. (2) using our NNSF ν predictions. The results are shown for different lower integration limits $x_{\text{min}} = 10^{-3}, 10^{-4}$ and for different nuclei $A = 1, 56$. For reference, we compare the NNSF ν calculations with the NLO fit to the CCFR data [17], the CERN-WA-047 measurements [18], and to the pure exact QCD predictions. All the results, except for the NNSF ν , are always the same in all the panels since they are independent of both x and A . In the case of the QCD predictions, the Q^2 dependence is entirely dictated by the running of the strong coupling $\alpha_s(Q^2)$. As in the previous section, the error bars on the NNSF ν represent the 68% confidence level intervals from the $N_{\text{rep}} = 200$ replicas fit.

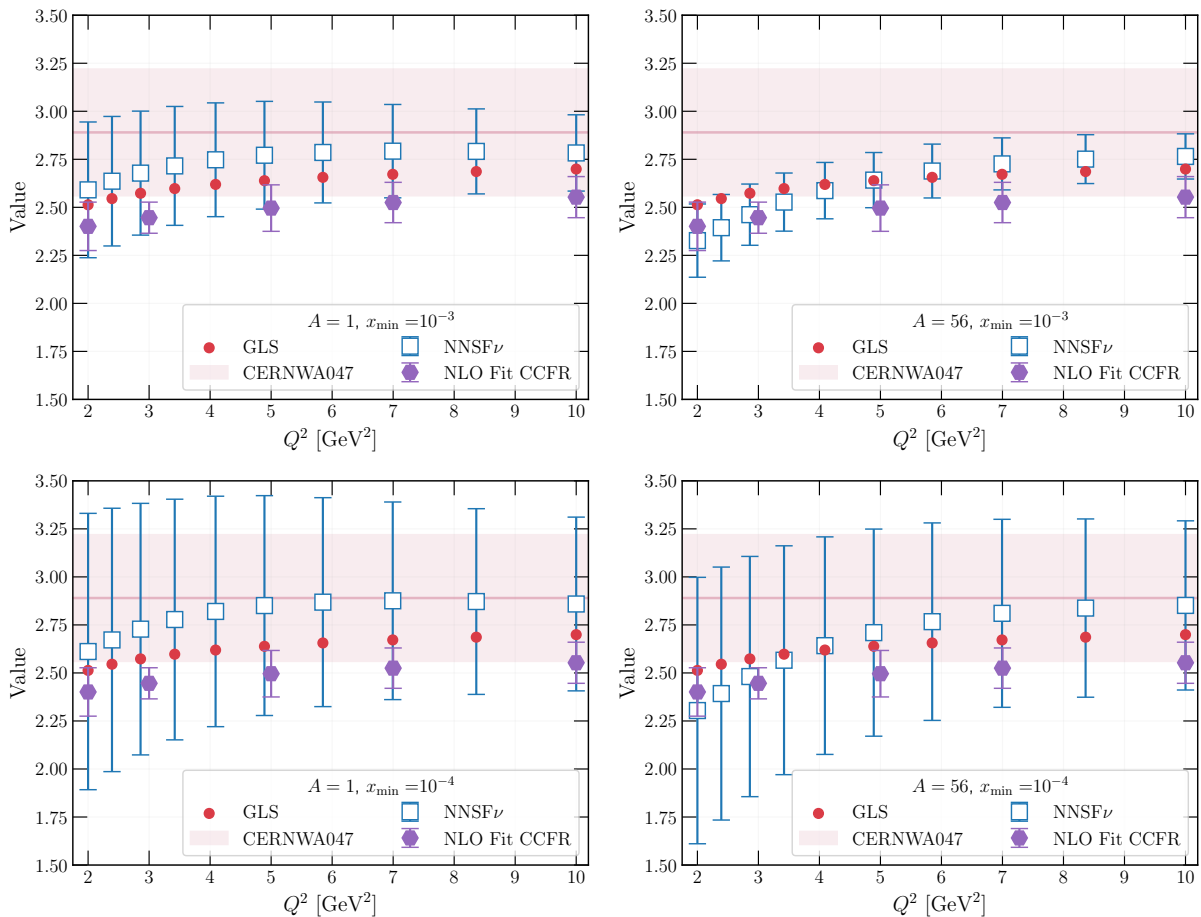


Figure 1: The GLS sum rule evaluated as a function of Q^2 . The NNSF ν predictions are compared with the NLO fit to the CCFR data (purple hexagons), the CERN-WA-047 measurements (red band), and to the pure QCD predictions (red dots). The results are displayed for different lower integration limits $x_{\min} = 10^{-3}$ (top) and of $x_{\min} = 10^{-4}$ (bottom panels), and for different atomic mass numbers $A = 1$ (left) and for $A = 56$ (right panels).

Based on these comparisons, we can conclude that there is in general good agreements between the different results. In particular, the NNSF ν and pure QCD predictions are in perfect agreement when the lower integration limit is taken to be $x_{\min} = 10^{-3}$. Even more remarkably, the slope of the GLS sum rule, which in the the QCD computation is purely dictated by the running of the strong coupling $\alpha_s(Q^2)$, is correctly reproduced by the NNSF ν predictions. The agreement in central values slightly worsens when the lower integration limit is lowered down to $x_{\min} = 10^{-4}$. Such a deterioration can also be seen in the increase of the uncertainties. As alluded earlier, such a behavior is expected due to the fact that NNSF ν does not have direct experimental constraints below $x \approx 10^{-3}$. Notice that the observations above hold for the different nuclei considered.

QCD effective charges. In order to fully understand the short- and long-range interactions, knowing the strong coupling α_s in the nonperturbative domain (or equivalently in the IR regime) is crucial. Further arguments can be put forth that knowing the IR-behavior of α_s is necessary to fully understand the mechanism for dynamical chiral symmetry breaking [9, 10]. However, studying the strong coupling in the IR domain is very challenging since standard perturbation theory cannot be used. In the following section, we explore an attempt to extend the perturbative domain using our NNSF ν framework to provide predictions for the low-energy strong coupling $\alpha_s(Q^2)$.

In the framework of perturbative QCD, the strong coupling – which at leading order can be approximated as $\alpha_s(Q^2) = 4\pi/\beta_0 \ln(Q^2/\Lambda^2)$ – predicts a diverging behavior at the Landau Pole when $Q^2 \rightarrow \Lambda^2$. Such a diverging nature is not an inconsistency of perturbative computations per se since the pole is located in a region way beyond the ranges of validity of perturbative QCD. Instead, the origin of such a divergence is the absence of nonperturbative terms in the series that cannot be captured by high order perturbative approximations. That is, the Landau singularity cannot be cured by simply adding more terms to the perturbative expansion. The Landau Pole however is unphysical (with the value of Λ^2 defined by the renormalization scheme) and this is supported by the fact that observables measured in the domain $Q^2 < \Lambda^2$ display no sign of discontinuity or unphysical behavior.

Several approaches have been explored to study the low-energy running of the coupling, each with its advantages, justifications, and caveats. A prominent approach based on Grunberg’s effective charge approach – that we attempt to pursue here – provides a definition of the coupling that behaves as α_s^{pQCD} at large- Q^2 but remains finite at small values of Q^2 . Since the regime is extended down to small- Q^2 , the effective charge incorporates nonperturbative contributions that appear as higher-twist. Such an effective charge is explicitly defined in terms of physical observables that can be computed in the perturbative QCD domain. An example of such observable that has been very well studied in the literature is the effective charge $\alpha_s^{\text{Bj}}(Q^2)$ defined from the polarized Bjorken sum rule [19, 20]. Such an observable has important advantages in that it has a simple perturbative series and is a non-singlet quantity implying that some Δ -resonance contributions cancel out.

In the following study, we use the effective charge $\alpha_s^{\text{GLS}}(Q^2)$ defined from the GLS sum rule introduced above. Following the Grunberg’s scheme, the definition of the effective charge $\alpha_s^{\text{GLS}}(Q^2)$ which follows from the leading order of Eq. (1) writes as:

$$\text{GLS}(Q^2, A) \equiv 3 \left(1 - \frac{\alpha_s^{\text{GLS}}(Q^2, A)}{\pi} \right) \iff \alpha_s^{\text{GLS}}(Q^2, A) = \pi \left(1 - \frac{\text{GLS}(Q^2, A)}{3} \right). \quad (3)$$

In the perturbative domain $\Lambda^2 \ll Q^2$, we expect the effective charges from the Bjorken and GLS sum rules to be equivalent $\alpha_s^{\text{GLS}}(Q^2) = \alpha_s^{\text{Bj}}(Q^2)$ up to $\mathcal{O}(\alpha_{\overline{\text{MS}}}^2)$. In addition, at zero momentum transfer we expect $\alpha_s^{\text{GLS}}(Q^2 = 0) = \alpha_s^{\text{Bj}}(Q^2 = 0) = \pi$. The latter kinematic limits originate from the fact that cross-sections are finite quantities and when $Q^2 \rightarrow 0 \Rightarrow x = Q^2/(2M\nu) \rightarrow 0$, the support integrand in Eq. (1) must also vanish; therefore we have the following relations:

$$\lim_{Q^2 \rightarrow 0} \text{GLS}(Q^2, A) = 0 \iff \alpha_s^{\text{GLS}}(Q^2 = 0) = \pi. \quad (4)$$

It is important to emphasize that Eq. (3) is directly related to the right-hand side of Eq. (1). We can see from this definition of the coupling that both the short-distance effects – those within the parentheses of Eq. (1) – and the long-distance perturbative QCD interactions – represented by the Δ^{HT} term– are incorporated into the expression of the effective coupling $\alpha_s^{\text{GLS}}(Q^2)$.

Fig. 2 displays the effective coupling $\alpha_s^{\text{GLS}}(Q)$ computed from the NNSF ν predictions. As for the sum rules, the effective charge is truncated at some values x_{min} in order to not be influenced by the small- x extrapolation region. The results are shown for $A = 208$ and for two different values of $x_{\text{min}} = 10^{-3}, 10^{-4}$. Our predictions are compared to the experimental measurements from JLab [11–14] which measures the Bjorken effective charge $\alpha_s^{\text{Bj}}(Q)$ using a polarized electron beam. Since the JLab results do not depend both on x and on the atomic mass number A , the results are the same for all the panels. This insensitivity of the results w.r.t the value of A reflects the expectation that both the

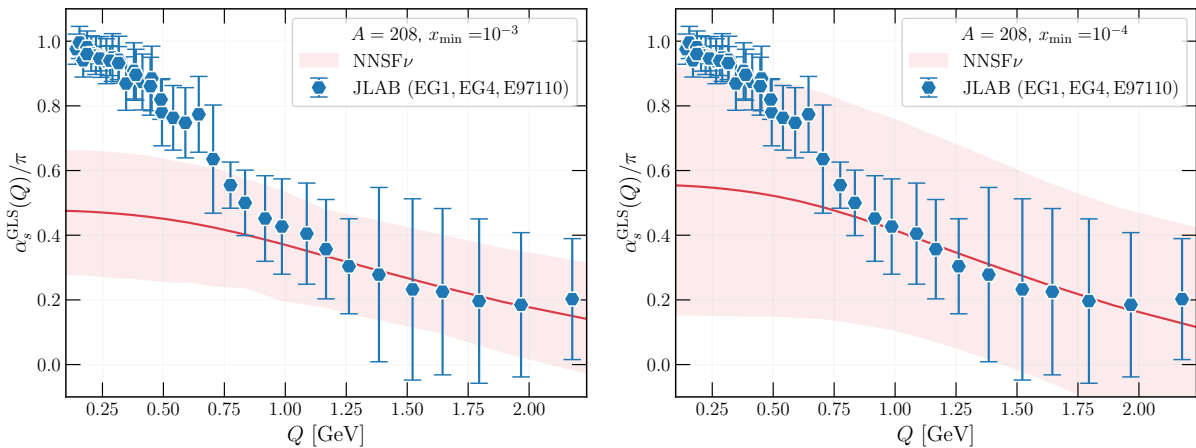


Figure 2: Effective charge defined in terms of the unpolarized GLS sum rule $\alpha_s^{\text{GLS}}(Q)$ computed from the NNSF ν predictions. The error bands represent the 68% confidence level intervals. The predictions are shown for two lower integration limits $x_{\text{min}} = 10^{-3}, 10^{-4}$. The results are compared to the measurements of the Bjorken effective charge $\alpha_s^{\text{Bj}}(Q)$ from JLab [11–14] (blue hexagons) with the error bars representing the statistical and systematic uncertainties summed in quadrature.

GLS and Bjorken sum rules are related to the nucleon valence sum rules and therefore take the same values irrespective of the value of A entering the calculations.

Based on these comparisons, we can infer that the NNSF ν predictions and the JLab experimental measurements agree very well down to $Q \sim 0.5$ GeV. As $Q \rightarrow 0$ we can see that the effective coupling $\alpha_s^{\text{GLS}}/\pi$ measured at JLab converges to 1 as per the kinematic limit while our predictions converges to $\sim \langle 0.6 \rangle$. Perhaps this result would slightly improve if the structure functions were forced to satisfy the sum rules during the fit and if more experimental measurements were available to constrain the small- x region. As before, the decrease in the value of the lower integration limit x_{min} induces a significant increase in the uncertainties.

Conclusions and outlook. In the first part of the manuscript, we reviewed a new framework – referred to as NNSF ν – for the determination of the neutrino-nucleus structure functions in the inelastic regime. In particular, we stressed on its capabilities to provide predictions for low-energy neutrino interactions. As a verification of the methodology, we compared the outcome of the computations of the GLS sum rule originating from such predictions with measured experimental data to which we found very good agreement.

In the second part, we used the NNSF ν determination as a tool to understand the running of the coupling $\alpha_s(Q^2)$ which encodes at the same time the perturbative dynamics at large momentum transfers and the nonperturbative dynamics underlying the color confinement at small momentum transfers. The use of standard perturbative computations to study the coupling at low- Q^2 yields erroneous results as it predicts a diverging behavior due to the existence of an unphysical pole. Owing to the lack of theoretical formalism that correctly accounts for the nonperturbative effects, studying the strong coupling in the IR regime is a challenging task.

A prominent approach that resolves the ambiguity in defining the strong coupling in the nonperturbative regime is the use of effective charges defined directly from a leading order perturbatively computable observable. In our study we defined the effective charge $\alpha_s^{\text{GLS}}(Q)$ from the GLS sum rule which at large momentum transfers reproduces the perturbative computations and at low momentum transfers is expected to converge to

π . Our predictions yield comparable results to experimental measurements – accounting for the uncertainties – down to $Q \sim 0.5$ GeV. However, our predictions do not fully satisfy the kinematic limit $\alpha_s(Q=0)/\pi = 1$ at zero momentum transfers. This issue of convergence might be resolved by imposing the neutrino structure functions to satisfy the sum rules during the fit. From this we conclude that further investigation is needed in that direction in order to fully understand the $Q \sim 0$ behavior.

Acknowledgments. The author is grateful to Juan Rojo for the careful reading of the manuscript. T. R. is supported by an ASDI (Accelerating Scientific Discoveries) grant from the Netherlands eScience Center.

References

- [1] U.-K. Yang and A. Bodek, *Parton distributions, d/u , and higher twist effects at high x* , *Phys. Rev. Lett.* **82** (1999) 2467–2470, [[hep-ph/9809480](#)].
- [2] A. Candido, A. Garcia, G. Magni, T. Rabemananjara, J. Rojo, and R. Stegeman, *Neutrino Structure Functions from GeV to EeV Energies*, *JHEP* **05** (2023) 149, [[arXiv:2302.08527](#)].
- [3] R. Abdul Khalek, R. Gauld, T. Giani, E. R. Nocera, T. R. Rabemananjara, and J. Rojo, *n NNPDF3.0: evidence for a modified partonic structure in heavy nuclei*, *Eur. Phys. J. C* **82** (2022), no. 6 507, [[arXiv:2201.12363](#)].
- [4] V. Bertone, R. Gauld, and J. Rojo, *Neutrino Telescopes as QCD Microscopes*, *JHEP* **01** (2019) 217, [[arXiv:1808.02034](#)].
- [5] **FASER** Collaboration, H. Abreu et al., *First Direct Observation of Collider Neutrinos with FASER at the LHC*, [arXiv:2303.14185](#).
- [6] **SND@LHC** Collaboration, R. Albanese et al., *Observation of collider muon neutrinos with the SND@LHC experiment*, [arXiv:2305.09383](#).
- [7] J. L. Feng et al., *The Forward Physics Facility at the High-Luminosity LHC*, *J. Phys. G* **50** (2023), no. 3 030501, [[arXiv:2203.05090](#)].
- [8] L. A. Anchordoqui et al., *The Forward Physics Facility: Sites, experiments, and physics potential*, *Phys. Rept.* **968** (2022) 1–50, [[arXiv:2109.10905](#)].
- [9] A. Deur, S. J. Brodsky, and G. F. de Teramond, *The QCD Running Coupling*, *Nucl. Phys.* **90** (2016) 1, [[arXiv:1604.08082](#)].
- [10] A. Deur, S. J. Brodsky, and C. D. Roberts, *QCD Running Couplings and Effective Charges*, [arXiv:2303.00723](#).
- [11] A. Deur et al., *Experimental study of isovector spin sum rules*, *Phys. Rev. D* **78** (2008) 032001, [[arXiv:0802.3198](#)].
- [12] **Resonance Spin Structure** Collaboration, K. Slifer et al., *Probing Quark-Gluon Interactions with Transverse Polarized Scattering*, *Phys. Rev. Lett.* **105** (2010) 101601, [[arXiv:0812.0031](#)].
- [13] A. Deur, Y. Prok, V. Burkert, D. Crabb, F. X. Girod, K. A. Griffioen, N. Guler, S. E. Kuhn, and N. Kvaltine, *High precision determination of the Q^2 evolution of the Bjorken Sum*, *Phys. Rev. D* **90** (2014), no. 1 012009, [[arXiv:1405.7854](#)].

- [14] A. Deur et al., *Experimental study of the behavior of the Bjorken sum at very low Q^2* , *Phys. Lett. B* **825** (2022) 136878, [[arXiv:2107.08133](#)].
- [15] D. J. Gross and C. H. Llewellyn Smith, *High-energy neutrino - nucleon scattering, current algebra and partons*, *Nucl. Phys. B* **14** (1969) 337–347.
- [16] X.-D. Huang, X.-G. Wu, Q. Yu, X.-C. Zheng, and J. Zeng, *The Gross-Llewellyn Smith sum rule up to $O(\alpha_s^4)$ -order QCD corrections*, *Nucl. Phys. B* **969** (2021) 115466, [[arXiv:2101.10922](#)].
- [17] A. L. Kataev and A. V. Sidorov, *The Gross Llewellyn-Smith sum rule: Theory VERSUS experiment*, in *29th Rencontres de Moriond: QCD and High-energy Hadronic Interactions*, pp. 189–198, 1994. [hep-ph/9405254](#).
- [18] **Aachen-Bonn-CERN-Democritos-London-Oxford-Saclay** Collaboration, T. Bolognese, P. Fritze, J. Morfin, D. H. Perkins, K. Powell, and W. G. Scott, *Data on the Gross-llewellyn Smith Sum Rule as a Function of q^2* , *Phys. Rev. Lett.* **50** (1983) 224.
- [19] J. D. Bjorken, *Applications of the chiral $u(6) \otimes u(6)$ algebra of current densities*, *Phys. Rev.* **148** (Aug, 1966) 1467–1478.
- [20] C. Ayala, G. Cvetič, A. V. Kotikov, and B. G. Shaikhatdenov, *Bjorken polarized sum rule and infrared-safe QCD couplings*, *Eur. Phys. J. C* **78** (2018), no. 12 1002, [[arXiv:1812.01030](#)].